

**Military Technical College
Kobry El-Kobbah,
Cairo, Egypt.**



**13th International Conference
on Applied Mechanics and
Mechanical Engineering.**

STUDY OF THERMOCAPILLARY EFFECTS IN TWO FLUID SYSTEMS USING A SINGLE PHASE MODEL

SAKR^{*} I.M., BALABEL^{**} A., HEGAB^{***} A.M. and SELIM^{****} S.M.

ABSTRACT

Thermocapillary flows within a differentially heated rectangular cavity containing two immiscible liquid layers are of considerable technological importance in materials processing applications particularly under microgravity conditions where the influence of buoyancy-driven convection is minimized. In the present study, for the first time, we account the affect of normal and tangential forces that control the track of the moving interface by using level set method (LSM). A 2-D numerical procedure for two immiscible fluid systems on the basis of a single phase model and the level set formulation is developed. The time dependent Navier-Stokes and energy equations are solved by means of the control volume approach on a staggered rectangular grid system. The numerical model interprets the tangential and the normal stresses by a single-phase model using a heavy side function. The topological change of the interface between the two immiscible flows is described by the level set method. According to our background this is the first study of such cases using the single phase model and the control volume formulation. Two cases have been studied: the first case contains a system with only one liquid interface (melt/encapsulant) between the two immiscible fluids. The second one has a system with encapsulant free surface opened to air (and so, subjected to a second thermocapillary forces). Both the liquid-liquid interface and the free surface are assumed to be initially flat, which is a valid assumption according to earlier theoretical and experimental results. In later cases, the liquid-liquid interface is allowed to deform. The numerical results are compared with the available analytical models and experimental results. The comparisons showed an acceptable agreement between the present predicted results and the available data shown in the available references.

KEY WORDS

Thermocapillary flow, Marangoni flow, two fluid systems, level set method.

* Lecturer, Dpt. of Mech. Power Eng., Faculty of Eng., Menoufiya Uni., Shebin El- Kom-Egypt.
** Lecturer, Dpt. of Mech. Power Eng., Faculty of Eng., Menoufiya Uni. Shebin El-kom-Egypt.
*** Assoc. Prof., Dpt. of Mech. Power Eng., Faculty of Eng., Menoufiya Uni., Shebin El- kom-Egypt.
**** Prof., Dpt. of Mech. Power Eng., Faculty of Eng., Menoufiya Uni., Shebin El-Kom- Egypt.

NOMENCLATURE

A	Aspect ratio, L/H_1	
Ca	Capillary number, $(\frac{\partial \sigma}{\partial T} \Delta T) / \sigma_{ref}$	
Cp	Specific heat,	j/kg.K
H	Total height of cavity (H_1+H_2)	
k	Thermal conductivity,	W/m.K
L	Length of cavity,	m
Ma	Marangoni number $\frac{\partial \sigma}{\partial T} \Delta T H_1^2 / (\mu_1 \alpha_1 L)$	
n	Normal vector	
Pr	Prandtl number, ν / α	
t	Tangential vector	
t, t*	Time, dimensionless time ,	sec
To	Reference temperature $T_h+T_c/2$,	K
T _c	Constant temperature at cold wall,	K
T _h	Constant temperature at hot wall,	K
u _{ref}	Reference velocity (α/H_1),	m/s
x	Horizontal distance,	m
X*	Dimensionless horiz. Coordinate ($=x/L$) or (x/H_1)	
y	Vertical distance,	m
Y*	Dimensionless vertical. Coordinate ($=y/L$) or (y/H_1)	

Greek Symbols

θ	Dimensionless temperature $(T-To)/(T_h-T_c)$	
σ	Surface tension,	N/m
ΔT	Maximum temperature difference $T_h - T_c$,	K
μ	Dynamics viscosity,	Pa.s
α	Thermal diffusivity $k/\rho C_p$,	m ² /s
β	Thermal expansion coefficient,	1/K
λ	Physicochemical parameter	
ν	Kinematic viscosity,	m ² /s
ρ	Density,	kg/m ³
ρ^*	Density ratio	
μ^*	Viscosity ratio	
α^*	Diffusivity ratio	

Subscripts

*	Relative quantities (layer 2 to layer 1)
i	i th fluid layer (i=1,2)

INTRODUCTION

The study of convective heat transfer in a system with more than one fluid is of interest to several engineering applications. To cite a few, metal casting operations, crystal growth methods, and the heat transfer phenomena occurring in day-to-day processes like the presence of air pockets in heat exchangers, water layers in multiple Layer glass windows, etc., involve the interaction of natural convection in immiscible fluids. The quest for making bigger and purer crystals for the electronics industry has led to adaptations and refinements of several terrestrial crystal fabrication methods to the microgravity environment of space. While the gravity effects are minimized on a space-based laboratory, surface tension effects are dominant at exposed free surface of a melt, and the resulting Marangoni or surface tension driven convection causes imperfections in a growing crystal. One of the ways of minimizing this Marangoni convection is the use of an encapsulant to seal off the melt-free surfaces. For example, in the Czochralski growth of Gallium Arsenide (GaAs), a liquid encapsulant like Boron trioxide, which is a high viscosity, low melting point glass, is used to reduce the surface tension driven flow and also used to prevent arsenic from evaporating and compromising the crystal stoichiometry. Similarly, in the float zone crystal growth method, liquid encapsulation has been used in obtaining striation-free silicon crystals in a microgravity environment. It is noted, that while the buoyancy forces reduced in space. They are nevertheless finite and involve strong temperature gradients. The modelling of such processes requires the understanding of the behaviour of system composed of immiscible fluids and the interaction of the various associated forces that control the system flow and heat transfer characteristics.

Villers and platten [1, 2], performed a one-dimensional (1-D) analysis of convective flow in a two-layer system. They assumed that the temperature gradient across the cavity is constant, and a parallel flow with negligible vertical velocity develops in both layers. By using the LDV technique (laser Doppler Velocimetry), Villers and Platten have also measured flow velocities in low speed thermal convective flows in single layers, and two-layer systems. Also for two-layer system in a cavity, Koster and Prakash [3], obtained experimental results including flow visualisation for the FC70-SiO₂S and FC70-SiO₂S systems.

Steady thermogravitational and thermocapillary driven flow of two immiscible liquid layers, subjected to a horizontal temperature gradient studied by Lui and Roux [4]. They assumed two-dimensional, incompressible, and unsteady flow. The governing equation is solved numerically by a finite difference method in a staggered grid. The shape of velocity profile is predicted and determined the number of convective cells through the two layers. Both situations with rigid or with free top surface have been considered. The computations have been performed for flat interfaces, liquid-liquid and liquid-gas. Most of them have been limited to a cavity of aspect ratio $A=2$ (length/height). The free surfaces were taken undeformable so that numerical results could be compared to analytical solution for infinite layers.

Ramachandran [5], investigated numerically the effects of buoyancy and surface tension gradient forces on thermal convection with two horizontal immiscible fluids subjected to an imposed lateral temperature gradient. The investigated flow system

consisted of a lighter fluid layer on top of a heavier fluid layer, and both layers were contained in a two-dimensional open cavity. Both upper free surface and the interface between the two fluid layers were assumed to be flat and undeformable in his calculations. Ramachandran solved the governing system of equations and boundary conditions by using a control volume –based finite difference scheme for two cases of immiscible fluids. The main results were for the steady-state calculations predicted dramatically different flows when interfacial tension effects were included, and complex flow patterns, with induced secondary flows, were found in both of the fluid layers.

Doi and Koster [6], investigated analytically and numerically two-dimensional pure thermocapillary convection in two immiscible fluid layers with an upper free surface. Both the free surface and the interface were assumed to be horizontal flat with zero deformation. The numerical study is performed Doi and Koster [6], to estimate the end wall effect in the case of the system of melt ($Pr=0.01$) and encapsulate ($Pr=1$) of equal depth. They derived an analytical solution in the steady state for infinite horizontal extent of the layers. Under a zero gravity environment, four different flow profiles exist which are controlled by a parameter, λ . This parameter is ratio of the temperature rate of change of the interfacial tension between the two layers to the temperature rate of change of the surface tension of the upper layer. They found three 'halt conditions' which stop the flow motion in the lower layer. The result identified the technologically relevant halt condition as $\lambda=0.5$. More over, they studied numerically the effects of the vertical end walls on the flow. The conditions of which the flow parameters above halt condition are predicted. It is found that for $0 < \lambda < 0.2$, thermocapillary convection can be greatly be suppressed in the encapsulated liquid layer at some higher Marangoni number.

Liu and Velarde [7], studied numerically two-dimensional thermocapillary convection in a system consists of two immiscible liquid layers subjected to a temperature gradient along their interface. The two-layer systems consist of: B_2O_3 (encapsulant) and GaAs (melt), for it experimental relevance in crystal growth by the directional solidification method. Two cases have been studied: a system with only one liquid interface (melt/encapsulant) and a system where the outer surface of encapsulant are open to air (and so, subject to a second thermocapillary force). Both the liquid-liquid interface and the outer surface are assumed to be undeformable and flat, which is a valid assumption according to earlier theoretical and experimental results. A 2-D numerical simulation of convection was carried out in a rectangular cavity by solving the system of Navier-Stokes equations using a finite difference method with a staggered grid for the pressure. Having in perspective a Spacelab experimentation they disregarded gravity ($g=0$). They show that a strong damping of a melt flow can be obtained by using an encapsulant liquid layer having appropriate viscosity, heat conductivity and /or thickness.

Liakopoulos, A. and Brown, G.W, [8], investigated numerically two dimensional thermocapillary convection in a cavity with differentially heated side walls. The governing equations with appropriate boundary and initial conditions are solved by a spectral element method. All numerical solutions are obtained using a time accurate integration scheme. They considered Reynolds and Prandtl numbers in the range: $Re \leq 1 \times 10^5$ for $Pr=0.01$ and $Re \leq 3 \times 10^3$ for $Pr=1$. They also considered buoyancy effects with Grashof number in the range $Gr \leq 1 \times 10^4$. The flexibility of the free surface is using the capillary numbers $Ca=0.05$ and 0.25 . The technique allowed distinguishing between

time independent and time oscillatory states. No oscillatory instability was encountered within the ranges of parameters that are covered in their studied.

Bethancourt L. and Hashiguchi [9], studied numerically the natural convection of a two-layer fluid a side-heated cavity. Two layers of immiscible Boussinesq liquids are contained in the enclosure. Numerical solutions are acquired to governing Navier-Stokes equations. No a priori assumptions are made on the shape and dynamical role of the interface. The impacts of a deformable interface and of surface tension are notable in local behaviour of heat transfer characteristics.

Ali Borhan et al. [10], studied numerically of thermocapillary convection in a rectangular cavity containing two horizontal immiscible fluid layers differentially heated from side in the absence of gravity. They are used domain mapping in conjunction with a finite-difference scheme on a staggered grid to solve for the temperature and flow fields while allowing the interface to deform. They used asymptotic solution and modified tangential stress. Interface deformations are small when the contact line of the interface is pinned on the solid boundaries. The flow pattern in the encapsulated layer and the resulting interface deformation are strongly dependent on both the thickness and the viscosity of the encapsulant layer.

H. Kohno and T. Tanahashi [11], studied numerical analysis of moving interface using a level set method coupled with adaptive mesh refinement in order to analyse moving interfaces. The finite element method is used to discretize the governing equations.

In order to track the movement of interface between two fluids, a number of methods have been developed. These methods are classified into two categories: the first one is the Volume of Fluid (VOF) Method and the second one is the Level Set Method (LSM). The latter has been used in a number of problems in applications including those in crystal growth, image processing and flame propagation, compressible and incompressible two phase flow [11]. In this method one defines a function $\phi(x, y, t)$, called level set that represent the interface at $\phi=0$. The level sets are advected by the local velocity field. The interface can be captured at any time by located the zero level set, which alleviates the burden of increasing grid resolution at the interface in many other numerical methods. The LSM provides convenient features for handling topological merging, breaking and self-intersecting of interfaces [12].

The present study is investigating the natural convection phenomenon in a stable system of immiscible fluids contained in an open and closed container. The geometry models the two-phase behaviour typical of many crystal growth and material processing techniques and is intended to provide insight into the system flow and thermal characteristics. The effect of surface tension at the interface and free surface with flat and deformable interface is considered. Moreover in this paper we present a single-phase level set method for viscous incompressible flow.

PHYSICAL MODEL AND GOVERNING EQUATIONS

A schematic of the geometry is shown in Fig.1. The system consists of two immiscible fluids and incompressible viscous fluids, liquid-2 (upper) and liquid-1(lower), in a two-dimensional cavity of length L and height H . The thickness of the upper layer is H_2 , and

that of the lower layer is H_2 , the total thickness is denoted H . The thickness ratio is $h^*=H_2/H_1$, and the lower-layer aspect ratio is $A=L/H_1$. The dynamic and kinematic viscosities, the density, the thermal conductivity and the thermal diffusivity of liquid-I are denoted $\mu_i, \nu_i, \rho_i, \alpha_i$ and κ_i respectively ($i=1, 2$). The rectangular cavity has a rigid bottom, a flat or d deformable liquid-liquid interface and two types of boundary condition for top surface :(1) rigid plate, and (2) free surface subject to thermocapillary effect. The vertical side walls of the cavity are maintained at constant temperatures T_h and T_c where $T_h > T_c$. The bottom and top walls are assumed to be adiabatic.

Our research studies have been based on a system of partial differential equations appropriate for the description of motion of the two immiscible fluids. These equations are well known as the equations for conservation of mass, momentum and heat equations for hydrodynamics. Although the force due to the surface tension acts on the interface boundary between the two layers, we found it convenient for the numerical simulation of the resulting mathematical model to include such surface force in the momentum equation. The moving interface satisfies a condition in the normal and tangential stresses between the two fluid which are $(\sigma \kappa n + \nabla_s \sigma)$, where n is a unit vector normal to the interface, κ is the curvature of the interface, σ is the surface tension which assumed to be function of temperature T and ∇_s denotes the surface gradient operator that can be written as $\nabla - \bar{n}(\bar{n} \cdot \nabla)$. Applying a Taylor series expansion of the surface tension about a reference temperature T_0 and keeping only the first two terms in such expansion, which is generally appropriate, we have

$$\begin{aligned} \sigma &= \sigma_{ref} - \gamma(T - T_0) \\ \nabla_s \sigma &= \sigma_T \nabla_s T \end{aligned} \tag{1}$$

where σ_{ref} is the value of the surface tension at the reference temperature and $\gamma = -d\sigma/dT$ evaluated at the reference temperature. Following the method of approach of Brackbill et al. [13], the surface tension force f_s can be incorporated into the momentum equation in the form.3

$$\begin{aligned} f_s &= (f_{sa}^n + f_{sa}^t) \delta(\phi) \\ f_{sa}^n &= \sigma \kappa n, \quad f_{sa}^t = \nabla_s \sigma \\ f_s^n &= (\sigma \kappa n_x + \sigma \kappa n_y) \delta(\phi) \\ f_s^t &= (\sigma_t \frac{\partial T}{\partial x} n_y - \sigma_t \frac{\partial T}{\partial y} n_x) \delta(\phi) \\ Ma_i &= -\sigma_T \frac{\Delta T H_1^2}{\mu_1 \alpha_1 L} \end{aligned} \tag{2}$$

where δ as the Dirac delta function, ϕ is a distance to the interface function and Ma_i is the Marangoni number corresponding to fluid1. Show the analysis of surface tension in Fig. 2. The system of partial differential equations under the present study then consists

of the equation (1), (2) and the following equations for the conservation of mass, momentum and heat, respectively:

$$\begin{aligned} \nabla \cdot \mathbf{u} &= 0 \\ \rho \left(\frac{\partial}{\partial t} + \mathbf{u} \cdot \nabla \right) \mathbf{u} &= -\nabla P + \nabla \cdot (\mu \nabla \mathbf{u}) + \mathbf{f}_s \\ \left(\frac{\partial}{\partial t} + \mathbf{u} \cdot \nabla \right) (\rho C_p T) &= \nabla \cdot (k \nabla T) \end{aligned} \quad (3)$$

where \mathbf{u} is the velocity vector, P is the pressure, μ is the dynamic viscosity, k is the coefficient of thermal conductivity, C_p is the specific heat and t is the time variable. The boundary conditions are as below.

$$\begin{aligned} u = v = 0 & \quad \text{at} \quad x = 0; x = L \\ u = v = 0 & \quad \text{at} \quad y = 0; y = H \\ \frac{\partial T}{\partial y} = 0 & \quad \text{at} \quad y = 0; y = H \\ T = T_H & \quad \text{at} \quad x = 0 \\ T = T_C & \quad \text{at} \quad x = L \\ & \text{at the interface (flat)} \\ v_1 = v_2 = 0 & \quad \text{at} \quad y = H_1 \\ T_1 = T_2 & \quad \text{at} \quad y = H_1 \\ & \text{if the free surface is flat} \\ \tau = \frac{\partial \sigma}{\partial T} \frac{\partial T}{\partial x} \\ Ma_2 = \left(-\frac{\partial \sigma_2}{\partial T} \right) \Delta T \frac{H_2^2}{L \alpha_2 \mu_2} \\ \lambda = \frac{\partial \sigma}{\partial T} / \frac{\partial \sigma_2}{\partial T} \end{aligned} \quad (4)$$

where Ma_2 is the Marangoni number corresponding to fluid 2 and λ is the physicochemical parameter. The equation was become in term of the level set function in the following to account for the 2 fluids. Where ϕ is a distance to the interface function, positive in liquid 1 and negative in fluid 2. The location of the interface is the given by the zero level set of the function ϕ , known as the level set function. The advection of the level set equation given by Osher and Sethian [14] is:

$$\frac{\partial \phi}{\partial t} + \mathbf{u} \cdot \nabla \phi = 0 \quad (5)$$

and from the level set function we can compute the normal as:

$$\mathbf{n} = \frac{\nabla\phi}{|\nabla\phi|} \quad (6)$$

The interfacial curvature κ is computed from

$$\kappa = \nabla \cdot \mathbf{n} \quad (7)$$

Since the fluid properties in Eq. (3) change discontinuously across the interface and the concentrated surface tension force also becomes infinite in an infinitesimal volume, direct solution of Eq.(3) is naturally difficult. Two approaches are usually followed to overcome these difficulties. In standard level set method, the interface is smoothed across a finite thickness region, usually a few grid point thick. The fluid properties and the delta function are thus modified as by Sussman et al [15],

$$\begin{aligned} \rho(\phi) &= \rho_1 + (\rho_1 - \rho_2)H(\phi) \\ \mu(\phi) &= \mu_1 + (\mu_1 - \mu_2)H(\phi) \end{aligned} \quad (8)$$

where $H(\phi)$ is the Heaviside function defined as:

$$H(\phi) = \begin{cases} 0 & \phi < -\varepsilon \\ \frac{1}{2} \left[1 + \frac{\phi}{\varepsilon} + \frac{1}{\pi} \sin\left(\frac{\pi\phi}{\varepsilon}\right) \right] & \phi \leq |\varepsilon| \\ -1 & \phi > \varepsilon \end{cases} \quad (9)$$

The interface thickness is approximately

$$\frac{2\varepsilon}{|\nabla\phi|} \quad (10)$$

where ε is a small distance from the interface. Thus the fluid properties are smoothed out in the normal direction of the interface over distance of ε on either side of the interface, making it a continuous function. Similarly a smooth delta function is defined as:

$$\delta(\phi) = \begin{cases} \frac{1}{2\varepsilon} \left[1 + \cos\left(\frac{\pi\phi}{\varepsilon}\right) \right] & \text{if } |\phi| \leq \varepsilon \\ 0 & \text{otherwise} \end{cases} \quad (11)$$

An important step is to maintain the level set function a distance function within the transition region at all times. This achieved by the Reinitialization step. More details about that will be given in Sussman et al. [15].

NUMERICAL PROCEDURE

The numerical procedure adopted here is essentially based on the finite volume method proposed by Patankar [16]. The well known SIMPLE algorithm is modified to account the level set method that follow the movements of the fluid/fluid interface. Moreover the modified algorithm is applied to resolve the pressure-velocity coupling in the momentum and energy equations. In the numerical schemes is convergence which is the combination of the level set method scheme. For more details about the numerical procedure and the consequence of the calculations, one can see Refs. [14], [15] and [17].

RESULT AND DISCUSSION

In this section, the numerical method described in the previous sections has been applied to three cases: thermocapillary a rigid top surface, thermocapillary a free top surface with flat interface and thermocapillary with deformable interface.

Thermocapillary with a Rigid Top Surface

Symmetrical system ($\mu^* = \alpha^* = 1$)

From the analytical expression of velocity profile in an infinite aspect ratio cavity with $g \neq 0$ (see viller et al. [1, 2]). Figure 3 indicates the velocity profiles for constant ratios of dynamics viscosity and thermal diffusivity. For high Ma the 2-D results tend to a parabolic evolution, in contrast with the linear 1-D solution. The results for horizontal velocity profile are compared with the analytical solution of Ref. [7]. In Fig.4, indicates the velocity Profiles for constant ratios of dynamics viscosity, thermal diffusivity and different Marangoni Number $100 \leq Ma_i \leq 1000$. It can be seen that, as the Ma_i increases velocity induced is also increased.

Effect of viscosity ratio μ^*

Figure 5 shows the velocity profile at $Ma_i = 1000$ for different viscosity ratios ($\mu^* = 0.1, 1, 10$). From Fig.5 it can be noticed that, the convective flow intensity in both layers diminishes when increasing the viscosity of the upper layer, for $Ma_i = 1000$.

The computed streamline and isothermal in the two layers are given for $\mu^* = 10$ in Fig.6. The case $\mu^* = 10$ (i.e., where encapsulate viscosity is greater than melt viscosity) fits better for crystal growth experiments as it corresponding to a reduced velocity in the melt. The case $\mu^* = 10$ streamline and isothermal in both layers are long symmetric with respect to the liquid-liquid interface. The Thermocapillary flow structure when $\mu^* = 0.1$ is shown in Fig.7 for $Ma_i = 1000$. A typical 'flywheel' structure appears in the upper layer near the cold end-wall, and a longer and larger convective cell fills almost all the melt layer. Even with so different structures, the two major convective cells have about the same intensity high.

Effect of thermal diffusivity ratios α^*

Now, let us vary only the thermal diffusivity of liquid -2(encapsulant) while of liquid -1 (melt) is maintained constant. For illustration, considered $\alpha_1=4.8 \times 10^{-7}$ and allowing $\alpha_2=(0.1 \text{ to } 10) \alpha_1$. Figure 8 shows the velocity profile at $Ma_i=1000$. It can be seen that the flow fields in each layer appear to be fully symmetric with respect to the interface. This is due to the fact that the Marangoni effects, which is the only driving force (along the interface), produces identical flow effects in the two layers. Indeed the viscous effect is the same in each layer (same viscosity, same geometry). Flow patterns together with isotherms are shown for $\alpha^*=0.1$ and $\alpha^*=10$ and $Ma_i=1000$, in Figs. 9 and 10, respectively. However, the thermal fields are different in the two layers (see Figs. 9 and 10.). The isotherm patterns change much more strongly in the liquid layer whose thermal diffusivity is weaker. However, as it can be seen in Fig.9, for $\alpha^*=0.1$, the 2-D numerical solution shows that the temperature distribution along the interface is strongly affected when the encapsulant has a lower diffusivity. The longitudinal temperature gradient decreases at the centre and increases near the end walls hence reducing convective flow in the system. For $\alpha^*=10$ (Fig.10.), the temperature gradient along the interface is more uniform.

Two fluid layer with actual properties

The Thermocapillary convection for a B_2O_3 (Boron trioxide)-GaAs (Gallium arsenide) system has been investigated for the aspect ratios ($A=L/H_1=4$). The physical properties of B_2O_3 -GaAs shown in table 1.

Figure 11 shows the horizontal velocity profiles at different Ma_i from (750 to 60000). It can be seen that, as The Marangoni number increases the velocity profile is also increased and symmetric. Figures 12a and 12b indicate the streamlines and isotherms in a ($A=4$) cavity for $Ma_i=1500$ and $Ma_i=6 \times 10^4$, respectively. In the two cases, two counter-rotating convective cells fill the whole cavity, one in each layer. The two cells have almost the same intensity for low Marangoni numbers. The form of the convective cell in the encapsulant almost does not change and that in the melt is significantly modified (with the cell centre moving towards the cold sidewall). At the same time, the change of the temperature field in the encapsulant is stronger than in the melt, due to the very high Prandtl number of the B_2O_3 liquid. The form of the concentrated convective cell ('flywheel' structure) occurring in the GaAs layer at $Ma_i=6 \times 10^4$ is similar to the one numerically found by Ref. [18] for a single liquid layer with a low-Prandtl-number ($Pr=0.0015$). Moreover, in our two-layer system, one may observe that the tendency of the flow towards the 'flywheel' structure in the melt is reduced relative to the case of a single liquid layer, due to the damping effect induced by the highly viscous B_2O_3 fluid. Thus both the high Prandtl number and the high viscosity of the encapsulant liquid drastically affect the Thermocapillary flow.

Thermocapillary with a Free Top Surface

The analytical expression of velocity profiles for a finite aspect ratio cavity with $g=0$ can be seen in (Doi et al. [6]), Where $\alpha^*=\alpha_2/\alpha_1$, $\mu^*=\mu_2/\mu_1$. The results for velocity profiles are compared with those of Doi et al. [6] in Fig.13a, and for temperature profile in Fig.13b. Both figures show a good agreement between the analytical solution and the numerical simulation. The key parameter of the figure is λ , which is considered for the ratio of Ma_i

at interface to Ma_2 at free surface. At $\lambda=0$, the interface velocity is negative, whereas, the surface velocity is positive. At $\lambda=0.5$, that "Halt condition" is reached in the lower encapsulated layer. At $\lambda=1$, the velocity profile in the upper layer shows two zero-velocity crossings which entails that two roll cells developed in the encapsulant layer. The temperature profiles reflect their coupling with the velocity profiles. On the other hand, it should be concluded that the analytical solution is only accurate for small temperature difference $\Delta T = T_{\text{hot}} - T_{\text{cold}}$.

Effect the encapsulant's viscosity

In this section, the system of B_2O_3 -GaAs with a highly viscous encapsulant in a wide range is considered, where, μ^* is taken as μ_2/μ_1 while keeping μ_2 constant. Figure 14 indicates that, for $\mu^*=1398$, damping of thermocapillary convection is strong in both encapsulant and melt layers. When decreasing μ^* by a factor 1000, thermocapillary convection becomes stronger in both encapsulant and melt layers, and the damping of the melt motion becomes weaker. The curve plotted in Fig.14 shows that the absolute interface velocity is nearly proportional to μ^* . In addition, these results show that even for the special situation when $\lambda=0.5$ (i.e. when thermocapillary forces at the encapsulant-melt surface and at the open, free top surface are balance). Thus a highly viscous encapsulant helps to strongly reduce motion in the melt. The effect of a highly viscous encapsulant can also be seen by comparing the flow structure at $\mu^*=1.398$ and at $\mu^*=1398$, see Fig.14, for $\mu^*=1.398$, the intermediate convection cell in the upper layer near the liquid-liquid interface appears and its intensity becomes much greater than that of $\mu^*=1398$, even for the special case of $\lambda=0.5$.

Thermocapillary with Deformable Interface

Let us consider a system of two immiscible and incompressible viscous fluids, in a two dimensional cavity of length L and height H as shown in Fig.1, The rectangular cavity has a rigid walls and the interface is assumed initially to be flat at $t=0$. However, for later times, the interface is allowed to deform according to the thermocapillary induced velocity components.

The present predicted interface deformation compared with the numerical results of Ref. [10] can be shown in Fig.15. At the beginning ($t=0$) the interface was assumed to be flat. By the time, deformation is observed in the interface. At high viscosity ratio the results indicate a similar behavior of the present and compared results, however at small viscosity ratio ($\mu^*=0.5$) there is a deviation between the two results near the cold wall. At $\mu^* > 1$, the lager pressure in the encapsulant layer near the cold wall causes the interface to dip into the melt, while the smaller pressure in the encapsulant layer near the hot end gives rises protrusion of the interface into the encapsulant layer. In contrary, when $\mu^* < 1$, the interface deformation gives a reverse behavior.

Figures 16 and 17 show the effect of viscosity ratio on the horizontal velocity and interface deformation. When the viscosity ratio decreases the absolute value of the velocity increases and there is a symmetric behavior in the velocity profile. When the viscosity of the upper layer is greater than that of the lower layer, the larger pressure in the encapsulant layer near the cold wall causes the interface to dip into the melt, while the smaller pressure in the encapsulant layer near the hot end gives rises protrusion of the interface into the encapsulant layer. In contrary, when the viscosity of the upper

layer is smaller than that of the lower layer, the interface deformation gives a reverse behaviour.

Two Fluid Layers with Actual Properties

The Thermocapillary convection for a B₂O₃ (Boron trioxide)-GaAs (Gallium arsenide) and Silicone oil (2 cSt)-silicone oil (0.65 cSt) system has been investigated for the aspect ratios ($A=L/H_1=4$). The physical properties of B₂O₃-GaAs shown in table 1 and Silicone oil (2 cSt)-silicone oil (0.65 cSt) shown in Table 2.

The midplane velocity and interface deformation for two-layer systems with different Marangoni number are presented in Figs. 18 and 19. As the Ma_i numbers are increased, the absolute of velocity at both the liquid-liquid interface and the absolute interface velocity increases. The effects of increasing Ma_i the interface deformation increase. At $\mu^* < 1$, the smaller pressure in the encapsulant layer near the cold wall causes the interface to rises protrusion into the encapsulant layer, while the lager pressure in the encapsulant layer near the hot end gives dip into the melt layer.

The midplane velocity and interface deformation for two-layer systems with different Marangoni number are presented in Figs. 20 and 21. As the Ma_i numbers are increased, the absolute of velocity at both the liquid-liquid interface and the absolute interface velocity increases. The effects of increasing Ma_i the interface deformation increase. At $\mu^* > 1$, the lager pressure in the encapsulant layer near the cold wall causes the interface to dip into the melt, while the smaller pressure in the encapsulant layer near the hot end gives rises protrusion of the interface into the encapsulant layer.

CONCLUSIONS

In this work, a numerical procedure for two immiscible flow simulations is developed. This kind of flows have several applications in general metal casting operations, crystal growth methods, and the heat transfer phenomena occurring in day-today processes like the presence of air pockets in heat exchangers, water layers in multiple Layer glass windows, chip encapsulation, etc., The numerical model interprets tangential and normal surface tension by level set methods that follow the moving deformable interface between two different fluids. The time dependent Navier-Stokes equations are solved by means of the control volume approach on a staggered rectangular grid system.

A numerical investigation of pure thermocapillary convection ($g=0$) has been carried out for two immiscible liquid layers in a rectangular cavity subjected to a temperature gradient parallel to the liquid-liquid interface. In the simpler case of rigid top boundary, a true cavity, the influence of viscosity ratio and diffusivity ratio of the two layers has been investigated for different orientation of two fluid systems. The unrealistic case of 'asymmetric' system with equal diffusivity and viscosity in each layer are considered; but with a temperature dependence on surface tension. In such cases, the flow structure and temperature fields are found to be perfectly symmetric with respect to the interface. For asymmetric systems with different thermal diffusivities ($\alpha_1 \neq \alpha_2$) but equal viscosity, the flow is symmetric while the temperature field is not. For asymmetric systems with different viscosities ($\mu_1 \neq \mu_2$), both velocity and temperature fields are

asymmetric. Increasing viscosity or reducing diffusivity in the encapsulant layer helps to reduce the convection intensity in the melt.

The experimentally relevant case of a B₂O₃ (Boron trioxide)-GaAs (Gallium arsenide) system was studied for two top surface conditions: either rigid or free but subject to thermocapillary forces. In case of free surface, a so called "halt condition" is obtained when $\lambda=0.5$, which stands for the ratio of the free surface's and the interface's Marangoni number. It is noted that, the use of highly viscous encapsulated layer reduce the intensity of thermocapillary convection in the melt.

The case of two immiscible liquid layers with deformed interface is examined for different aspect-ratios of two layers and a wide range of the dynamics parameters. The flow pattern in the encapsulated layer is strongly dependent on both the thickness and the viscosity of the encapsulant layer. Interface deformations are found to be small when the contact lines of the interface are pinned on the solid boundaries. The higher viscosity of the encapsulant layer gives rise to a larger pressure gradient in that layer, thereby resulting in interface deformations. The numerical results are compared with the available analytical models and experimental results. The comparisons showed an acceptable agreement between the present predicted results and the available data shown in the previous references.

REFERENCES

- [1] D.Villers and J.K Platten," Thermal convection in Superposed Immiscible liquid layers", App.Scient.REs.45, pp.145-152, (1988).
- [2] D.Villers and J.K Platten., " Influence of interfacial tension gradients On Thermal convection in two superposed immiscible liquid Layers", App. Scient. Res.47, pp. 177-191, (1990).
- [3] A. Prakash and J.N. Koster," Convection in multiple layers of immiscible liquids in a shallow cavity-II", Int.J.Multiphase Flow, 20, pp.397- 414, (1994).
- [4] Q.S. Liu and B. Roux, "Thermogravitational and Thermocapillary Convection in a cavity containing two superposed immiscible liquid Layers", Int. J. Heat and Mass Transfer, 36, pp.101-117, (1993).
- [5] N. Ramachandran, "Thermal Buoyancy and Marangoni Convection In Two Fluid Layered System", J. Thermophysics and heat Transfer, 7, pp. 352-36, (1993).
- [6] T. Doi and J.N. Koster, "Thermocapillary convection in two immiscible Liquid layers with free surface ", Phys.Fluids, 5, pp.1914-1927, (1993).
- [7] Q.S. Liu and M.G Velarde, "Thermocapillary Convection in two-layer systems", Int. J. Heat Mass Transfer, 41, pp.1499-1511, (1998).
- [8] A. Liakopoulos and G.W. Brown, "Thermocapillary and natural Convection in a square cavity", AMD, 170, pp.57-74, (1993).
- [9] A.M. Bethancourt L. and K. M. Hashiguchi, "Natural Convection in a two-Layer fluid in a side-heated cavity", Int. J. Heat Mass Transfer, 42, pp. 2427-2437, (1999).
- [10] N.R. Gupta, H. Haj - Hariri, and Ali Borhan, "Thermocapillary flow in a double-layer fluid structures: An effective single-layer Model", J. Colloid and Interface Science, 293, pp.158-171, (2006).

[11] Haruhiko Kohno and Takahiko Tanahashi, "Numerical analysis of moving interfaces using a level set method coupled with adaptive mesh refinement", Int. J. Numer. Meth. Fluids, 45, pp.921-944, (2004).

[12] W. Mulder, S. Osher and J.A. Sethian, "Computing interface Motion in compressible gas dynamics ", J.Comput.Phys.100, pp209-228, (1992).

[13] J.U. Brackbill, D.B. Kothe and C. Zemach,"A Continuum Method for Modeling Surface Tension ", Journal of Comput. Physics, 100, 335-354, (1992).

[14] S. Osher and J.A. Sethian," Front Propagation with Curvature Dependent speed Algorithms based on Hamilton-Jacobi Formulation", J. Computatinal Physics, 79, pp.12-49(1988).

[15] M. Sussman, P. Smereka and S. Osher, "A level set approach for Computing solutions to incompressible two-phase Flow", J. Comput.Phys.114, pp.146-159, (1994).

[16] S.V. Patankar, "Numerical Heat Transfer and Fluid flow", McGraw- Hill, New York. (1980). (Book)

[17] A. Hegab, T.L. Jackson, J. Buckmaster, and D. S. Stewart, "Nonsteady Burning of Periodic Sandwich Propellants with Coupling the Solid and Gas Phases", Combustion and Flame,125,pp1055-1070,. (2001).

[18] H. Ben Hadid and B. Roux , "Thermocapillary Convection in long horizontal layers a low-Prandtl-number melts Subject to a horizontal temperature gradient", J.Fluid Mech., 221, pp.77-103, (1990).

[19] E.T. Tudose, "An Experimental study of Buoyant thermocapillary convection in a rectangular cavity", Ph.D, Ap.Chem. Uni. Of Toronto,(2002).

Table1. Physical properties of the B₂O₃ liquid and the GaAs liquid in Ref. [7].

Fluid	α [m ² /s]	k[W/m/k]	μ [Kg/m s]	ν [m ² /s]	ρ [Kg/m ³]	B[1/k]	Pr
GaAs	7.17x10 ⁻⁶	17.8	2.79x10 ⁻³	4.9x10 ⁻⁷	5720	1.87x10 ⁻⁴	0.068
B ₂ O ₃	2.52x10 ⁻⁶	2	3.9	2.37x10 ⁻³	1648	9.0x10 ⁻⁵	939.1
B ₂ O ₃ / GaAs	0.352	0.112	1398	4829	0.288	0.481	13741

Table2. Physical properties of the 0.65 cSt liquid and the 2 cSt liquid in Ref. [19]

Fluid	α [m ² /s]	k[W/m/k]	μ [Kg/m s]	ν [m ² /s]	ρ [Kg/m ³]	B[1/k]	Pr
2 cSt	0.8x10 ⁻⁷	0.12	1.75x10 ⁻³	2x10 ⁻⁶	873	0.00117	27
0.65 cSt	0.77x10 ⁻⁷	0.1	4.927x10 ⁻⁴	0.65x10 ⁻⁶	758	0.00134	8.2
0.65cSt/ 2cSt	0.9625	0.112	0.2815	0.325	0.868	1.145	0.303

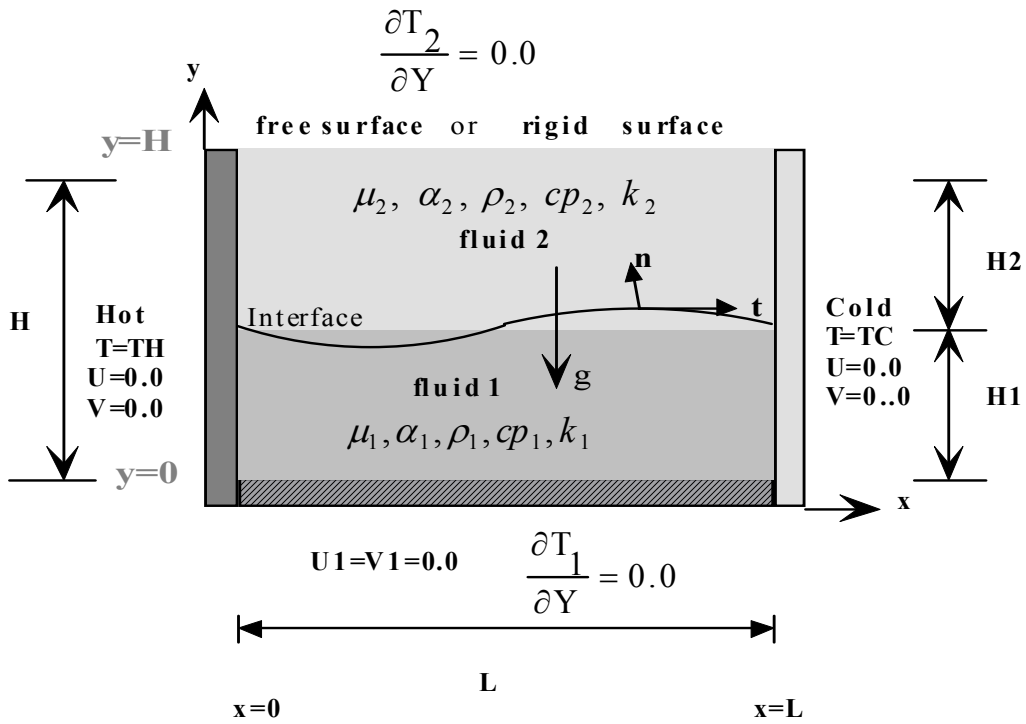


Fig.1. Schematic of the physical setup.

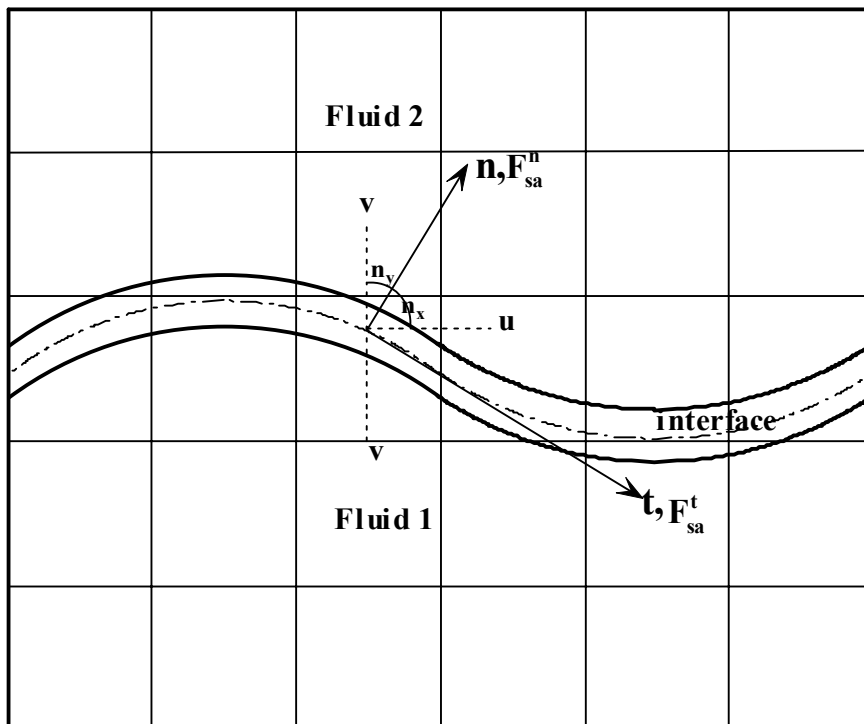


Fig.2. A Schematic of Two-layer problem with deformable interface.

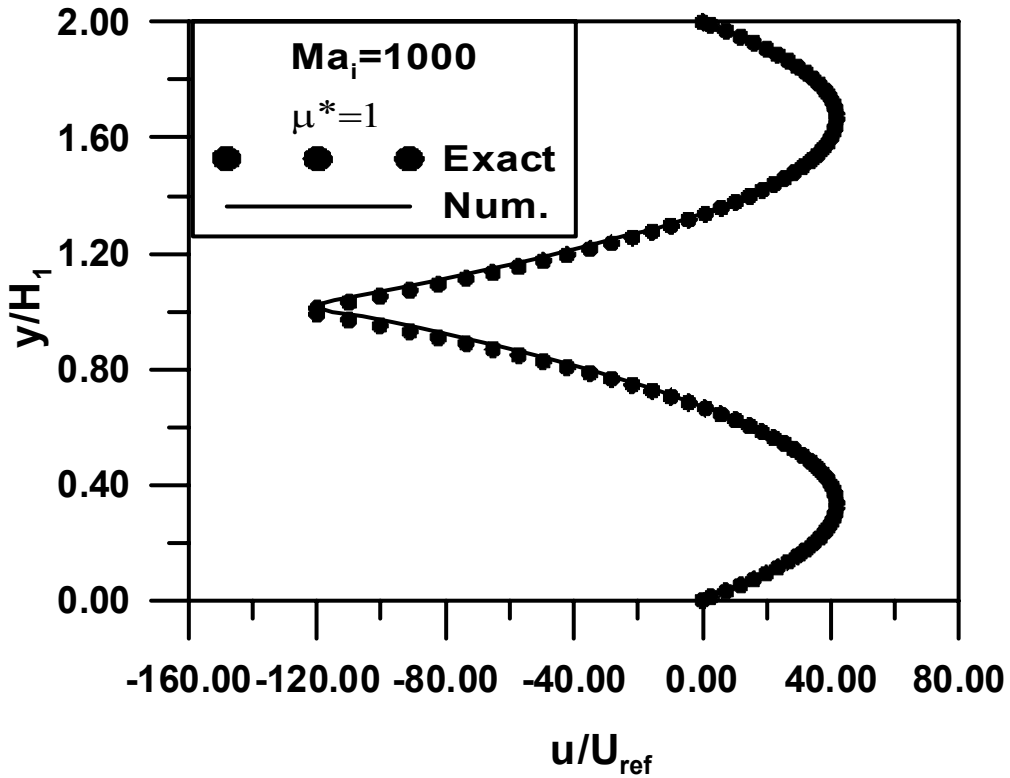


Fig.3. Horizontal velocity at $x^*=A/2$ for $Ma_i=1000$, $Pr_1=Pr_2=1$, $H^*=\mu^*=\alpha^*=\rho^*=k^*=1.0$ and $A=L/H_1=4.0$.

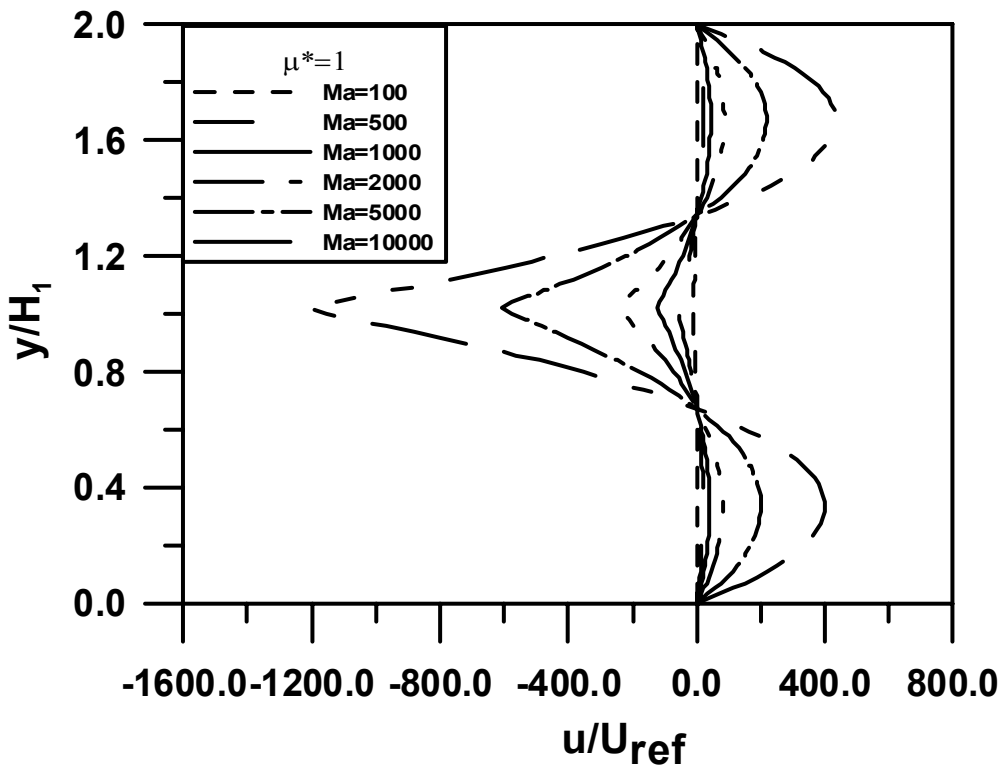


Fig.4. Horizontal velocity at $x^*=A/2$ for $Pr_1=Pr_2=1$, $H^*=\mu^*=\alpha^*=\rho^*=k^*=1.0$ and $A=L/H_1=4.0$.

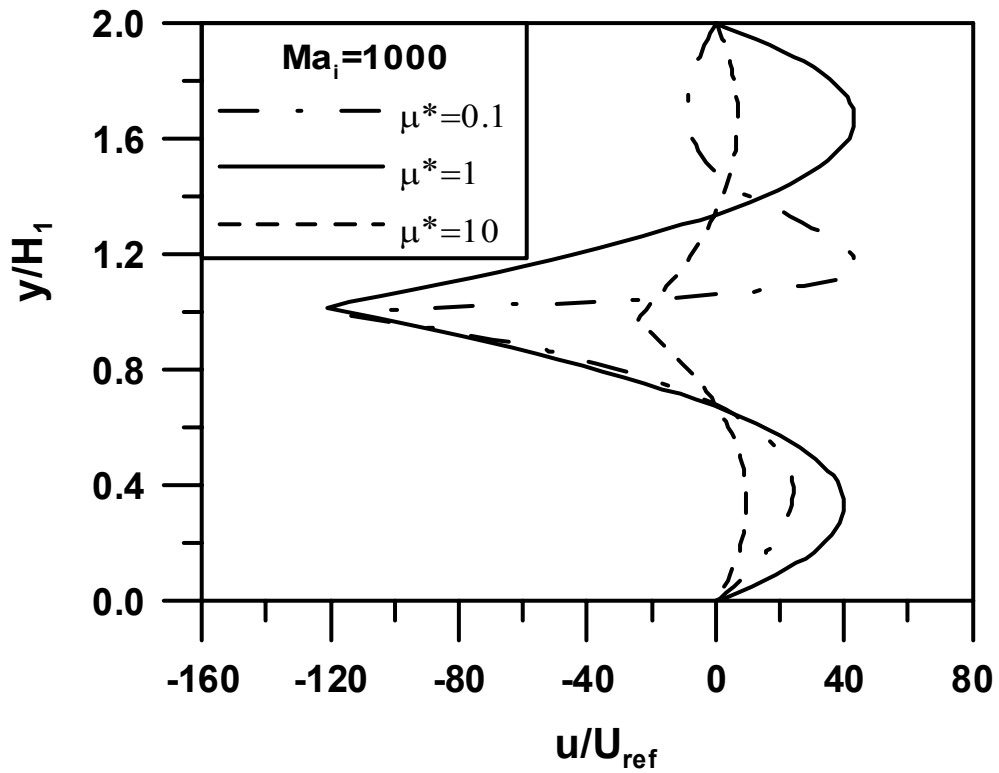


Fig.5. Horizontal velocity at $x^*=A/2$ for $Ma_i=1000$, $Pr_1=H^*=\alpha^*=k^*=1.0$ and $A=L/H_1=4$.

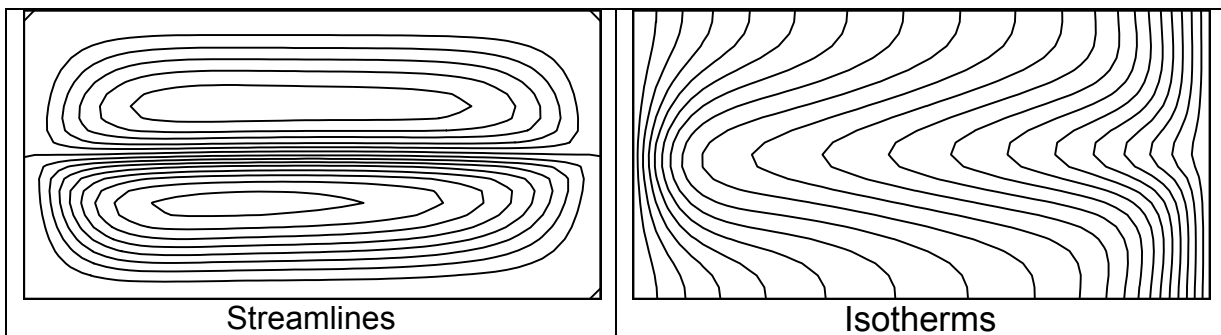


Fig.6. Streamlines and isotherms for asymmetric system $\mu^*=10$, $Ma_i=1000$, $Pr_1=H^*=\alpha^*=k^*=1.0$ and $A=L/H_1=4$.

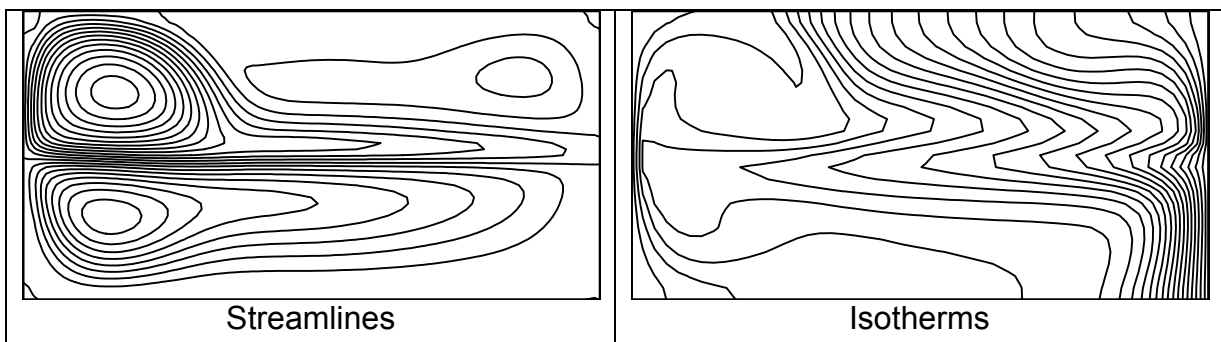


Fig.7. Streamlines and isotherms for asymmetric system $\mu^*=0.1$, $Ma_i=1000$, $Pr_1=H^*=\alpha^*=k^*=1.0$ and $A=L/H_1=4$.

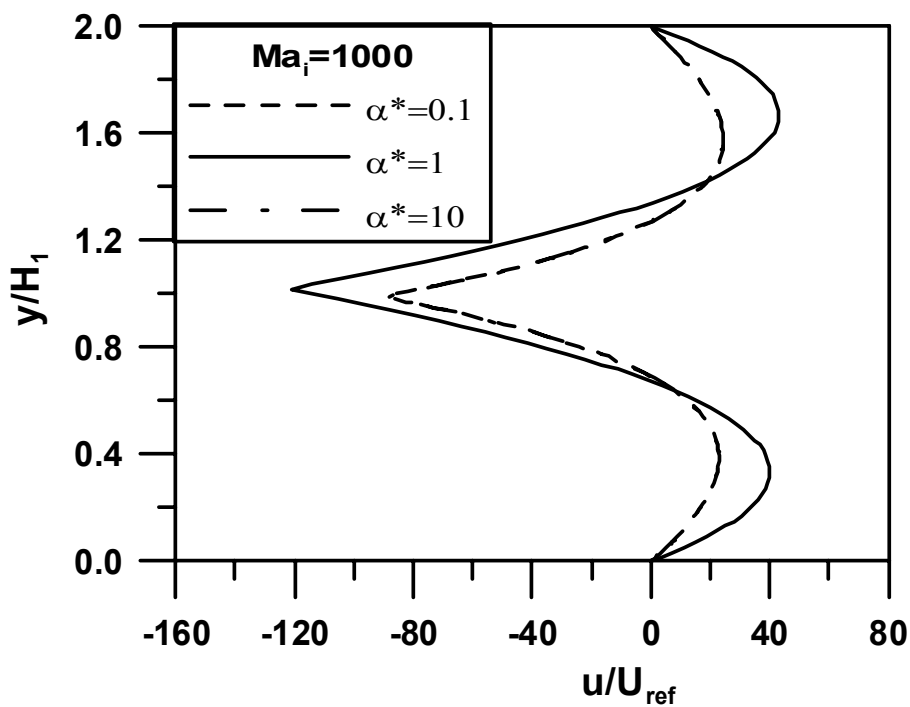


Fig.8. Horizontal velocity at $x^*=A/2$ for $Ma_i=1000$, $Pr_1=H^*=\mu^*=k^*=1.0$ and $A=L/H_1=4$.

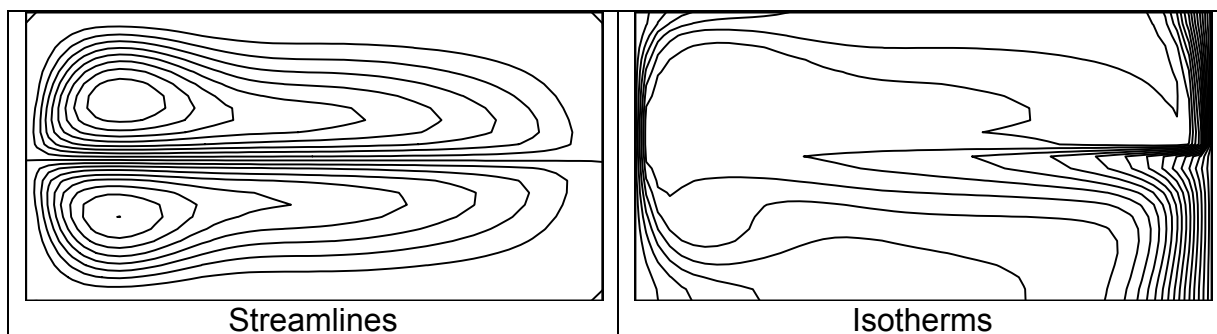


Fig.9. Streamlines and isotherms for asymmetric system $\alpha^*=0.1$, $Ma_i=1000$, $Pr_1=H^*=\mu^*=k^*=1.0$ and $A=L/H_1=4$.

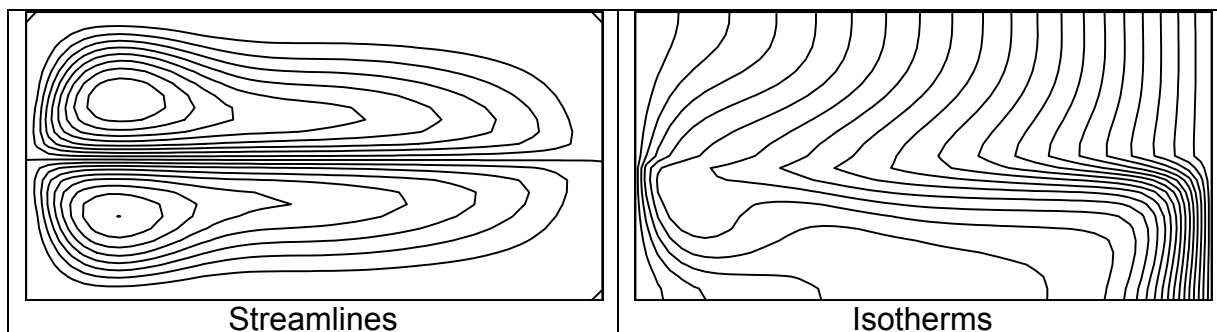


Fig.10. Streamlines and isotherms for asymmetric system $\alpha^*=10$, $Ma_i=1000$, $Pr_1=H^*=\mu^*=k^*=1.0$ and $A=L/H_1=4$.

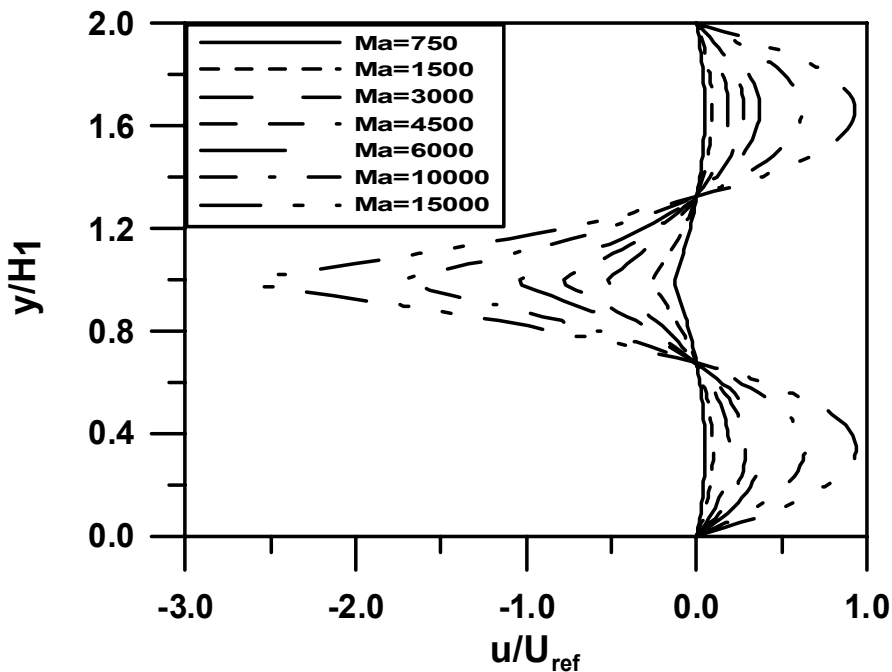


Fig.11. Horizontal velocity at $x^*=A/2$ for different Ma_i at $Pr_1=0.068$, $H^*=1$, $\mu^*=1398$, $k^*=0.112$, $\alpha^*=0.352$, $A=L/H_1=4.0$.

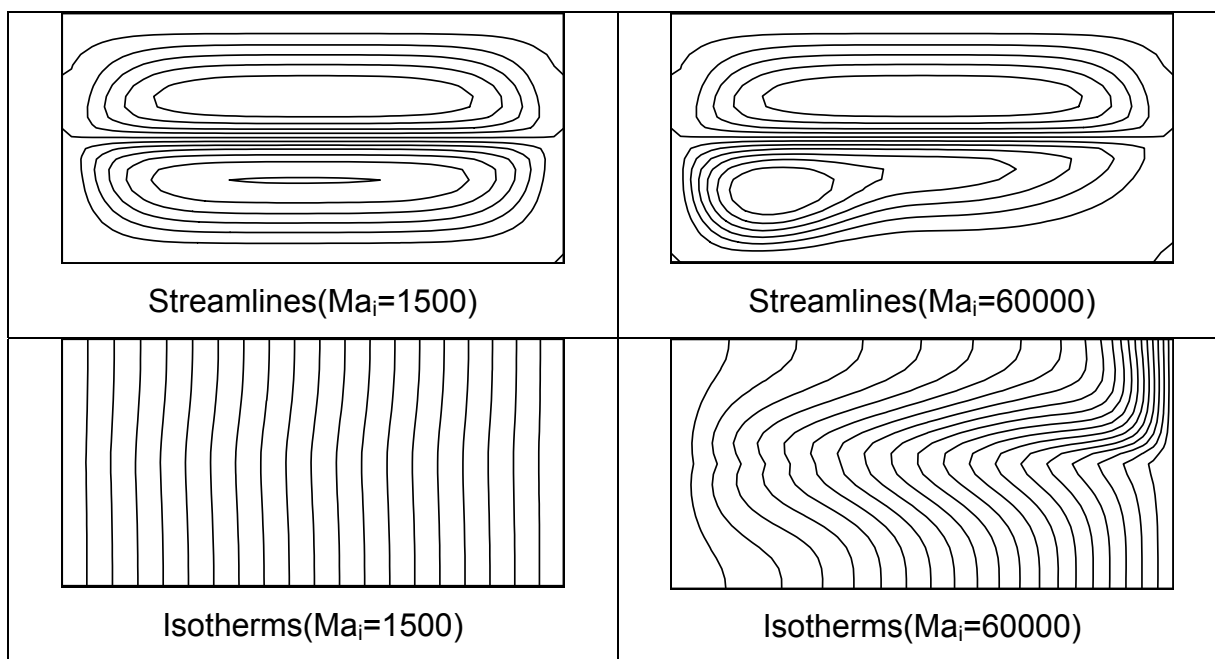
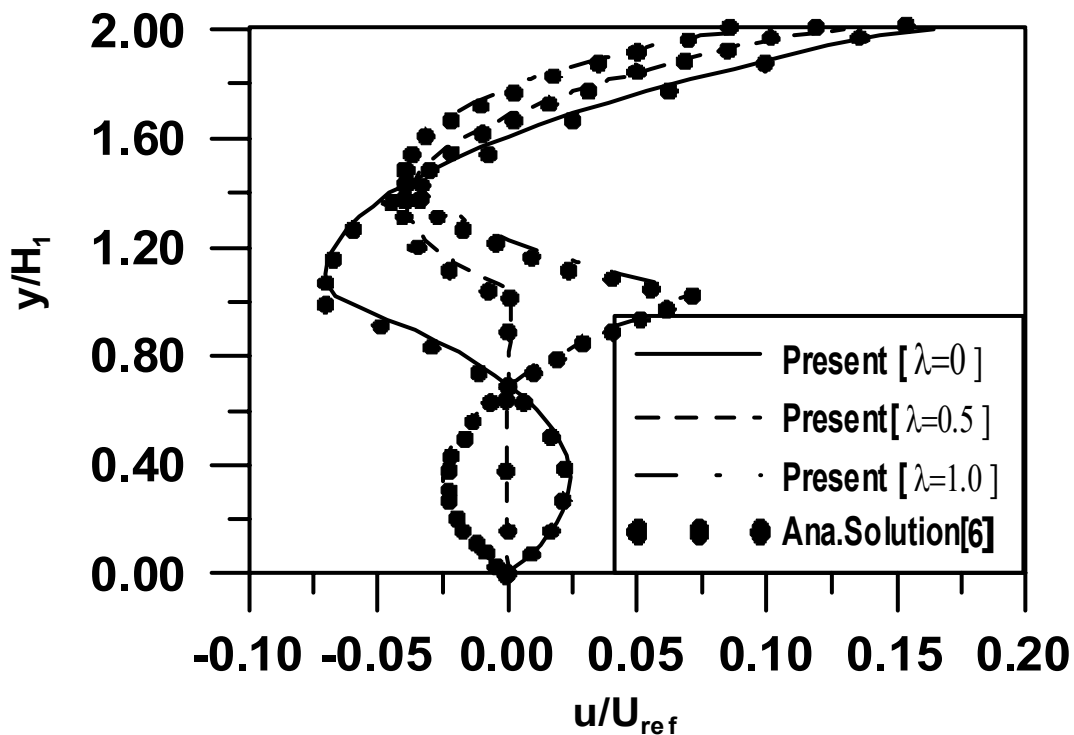
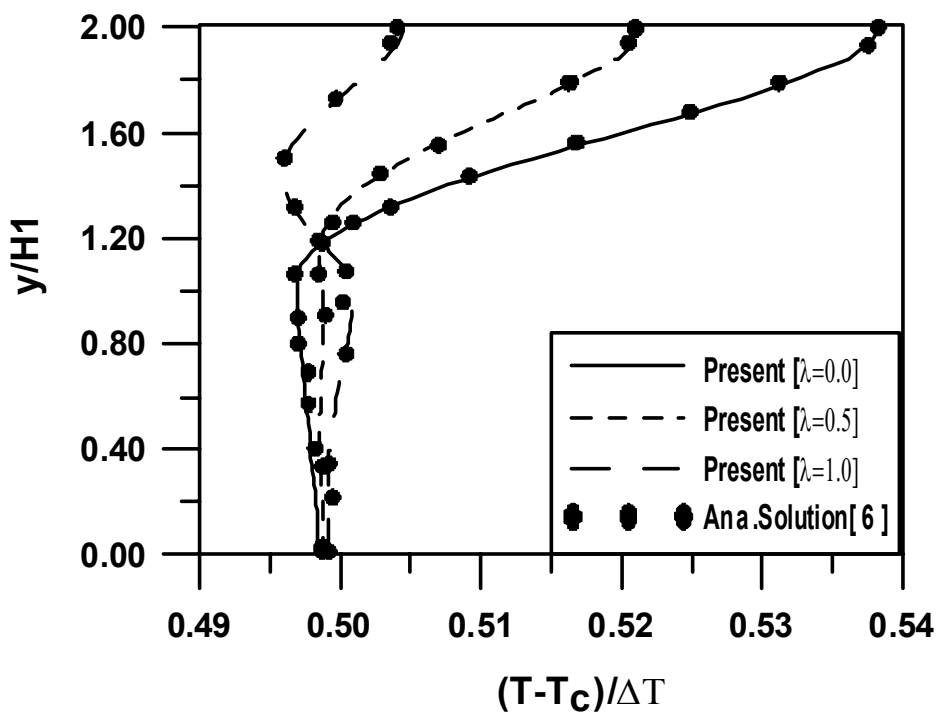


Fig.12. Streamlines (above) and isotherms (below) for asymmetric system for $A=L/H_1=4.0$, $H^*=1$ at: (a) $Ma_i=1500$ and (b) $Ma_i=60000$.



(a)



(b)

Fig.13. (a) Horizontal velocity profiles on $X^*=2$, (b) Temperature profile at $X^*=2$, for $Pr_1=0.01$, $Pr_2=1.0$, $\alpha^*=0.1$, $\mu^*=10$, $Ma_2=5.0$ at $A=L/H_1=4.0$.

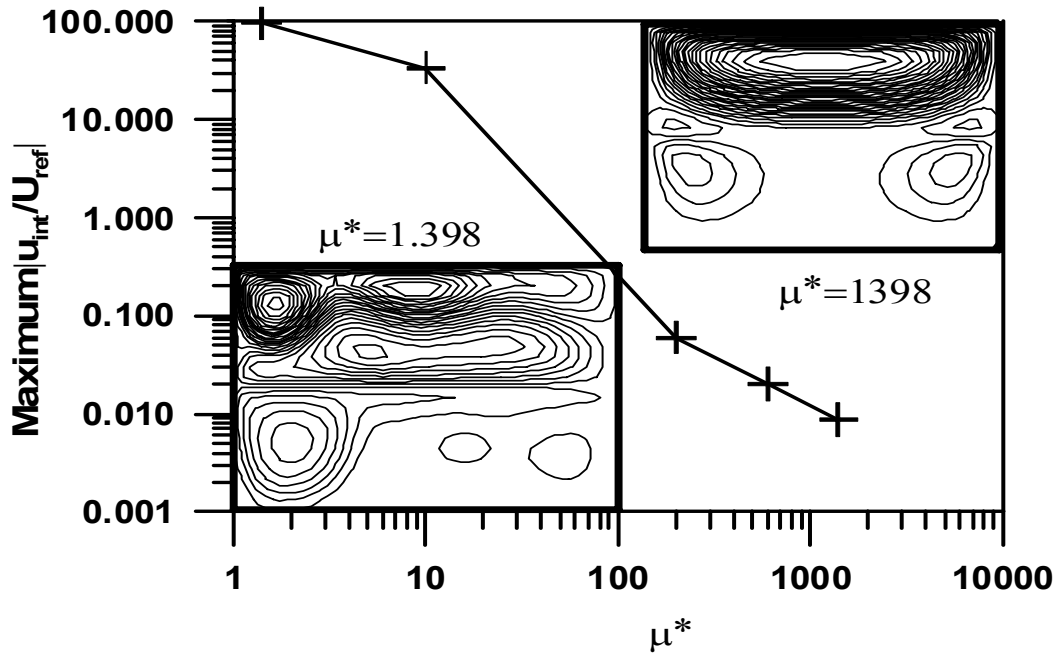
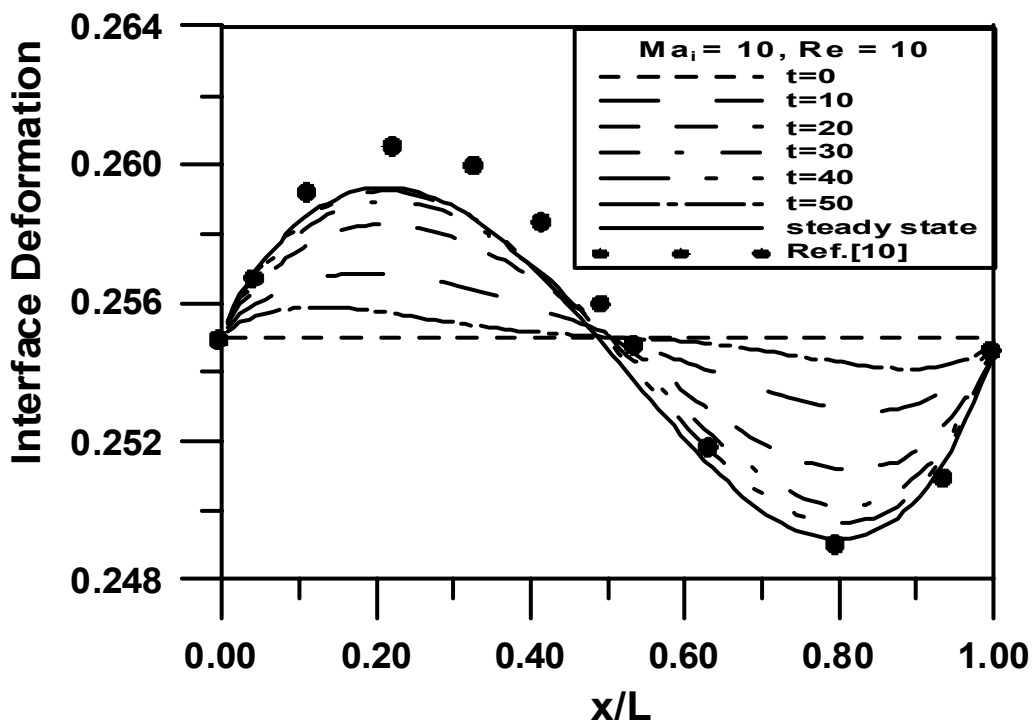


Fig.14. Maximum Absolute interface velocity at $X^*=A/2$, as function of μ^* , and two typical flow structures at $\mu^*=1398$ and $\mu^*=1.398$, for free surface at $A=L/H_1=4.0$, $Ma_i=3750$, $\lambda=0.5$.



(a)

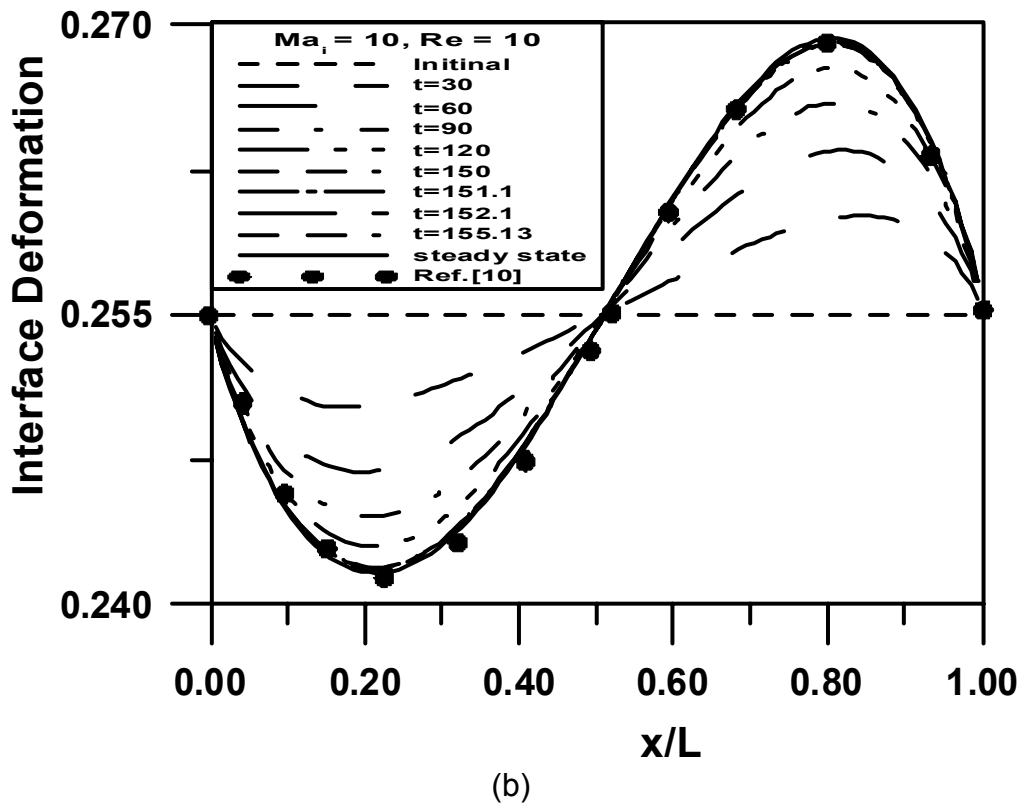


Fig.15. Interface Deformation with $Ma_i=10, Re=10, Pr=1, k^*=1.0$: (a) $\mu^*=0.5, A=H/L=1$
 (b) $\mu^*=10, A=H/L=0.5$.

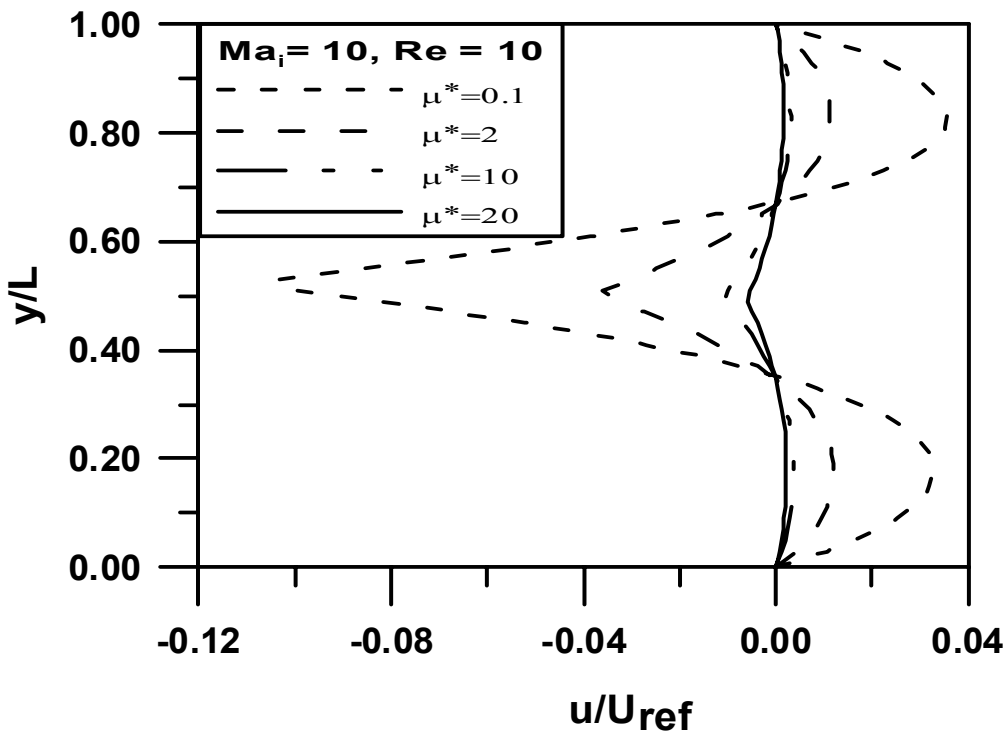


Fig.16. Horizontal velocity at different viscosity ratios of encapsulant phases, $X^*=L/2$, with $Pr_1=1, Ma_i=10, \alpha^*=1, k^*=1$ and $A=H/L=1$.

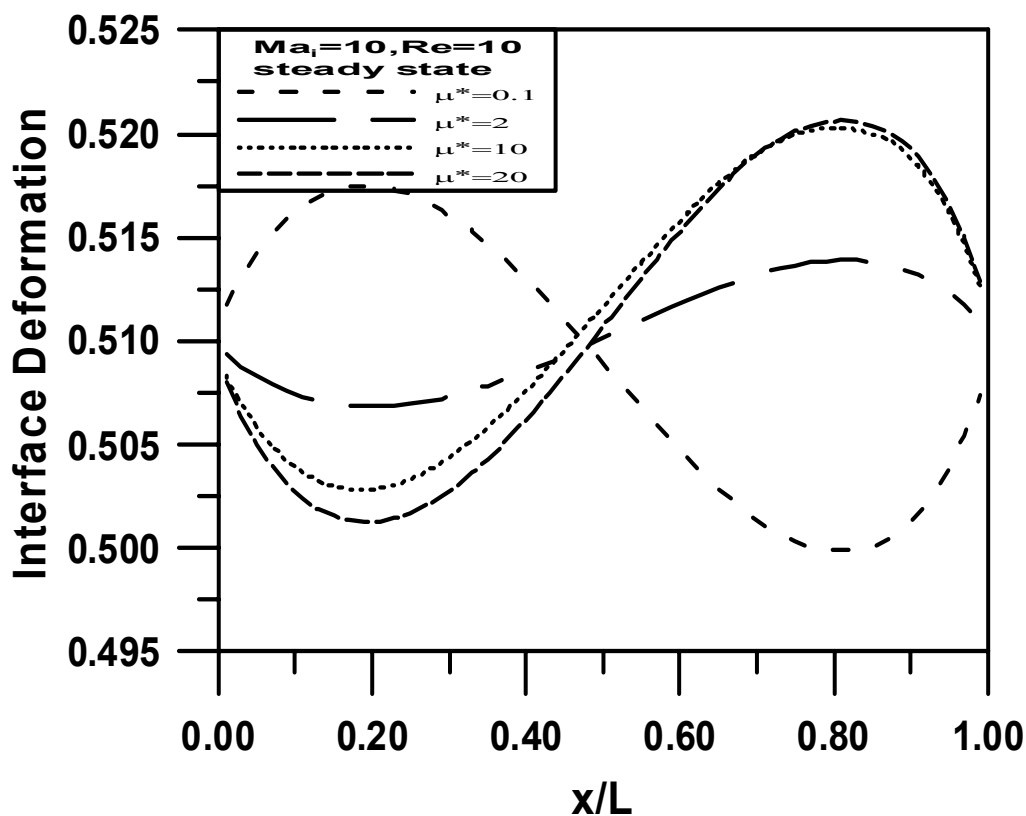


Fig.17. Interface Deformation with $Ma_i=10$, $Re=10$, $Pr=1$, $\mu^*=k^*=1.0$ and $A=H/L = 1$.

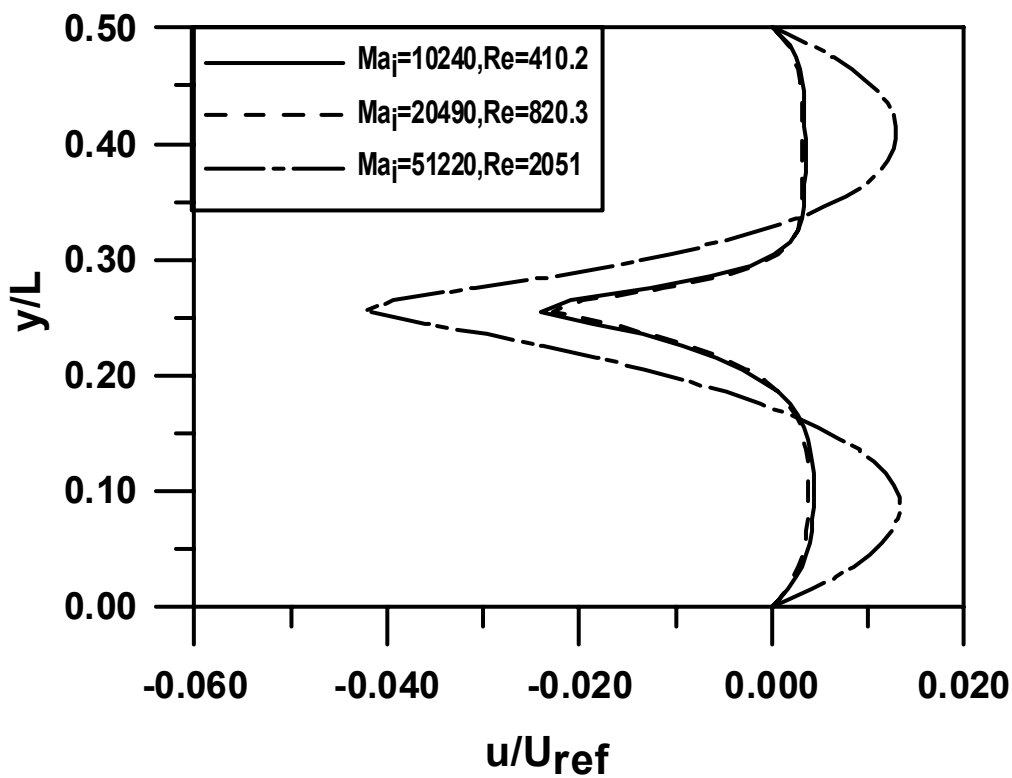


Fig.18. Horizontal velocity at $x^*=A/2$ for different Ma_i at $A=L/H = 2.0$.

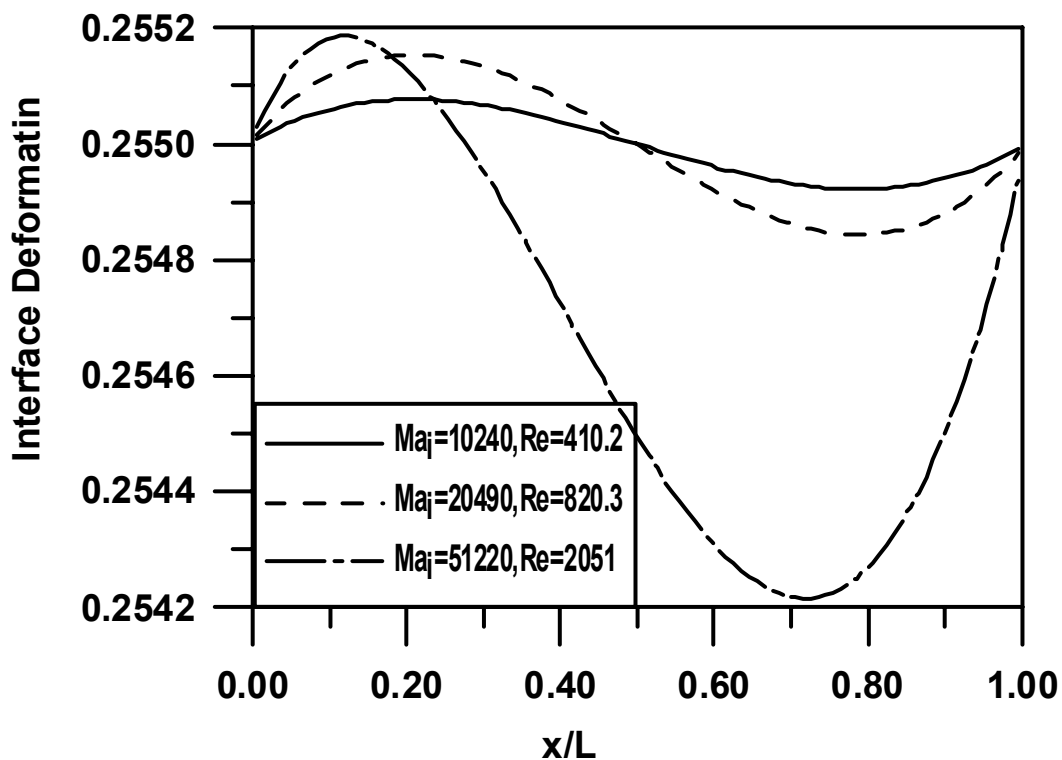


Fig.19. Interface deformation for different Ma_i at A=L/H=2.0.

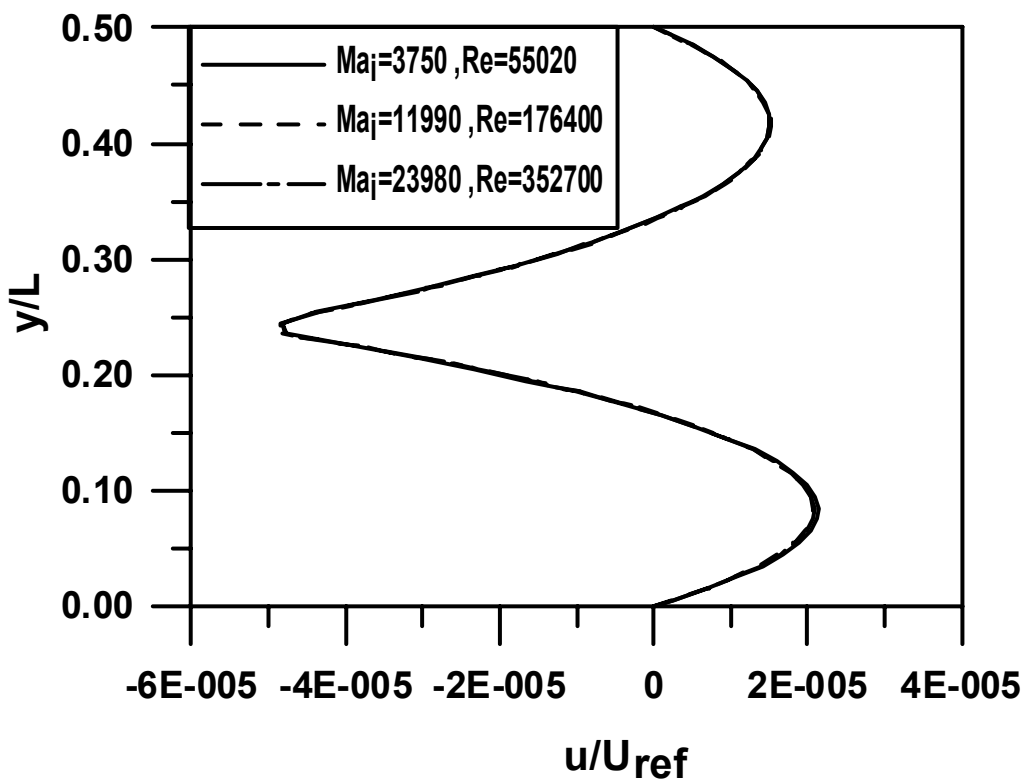


Fig.20. Horizontal velocity at x^{*}=A/2 for different Ma_i at A=L/H=2.0.

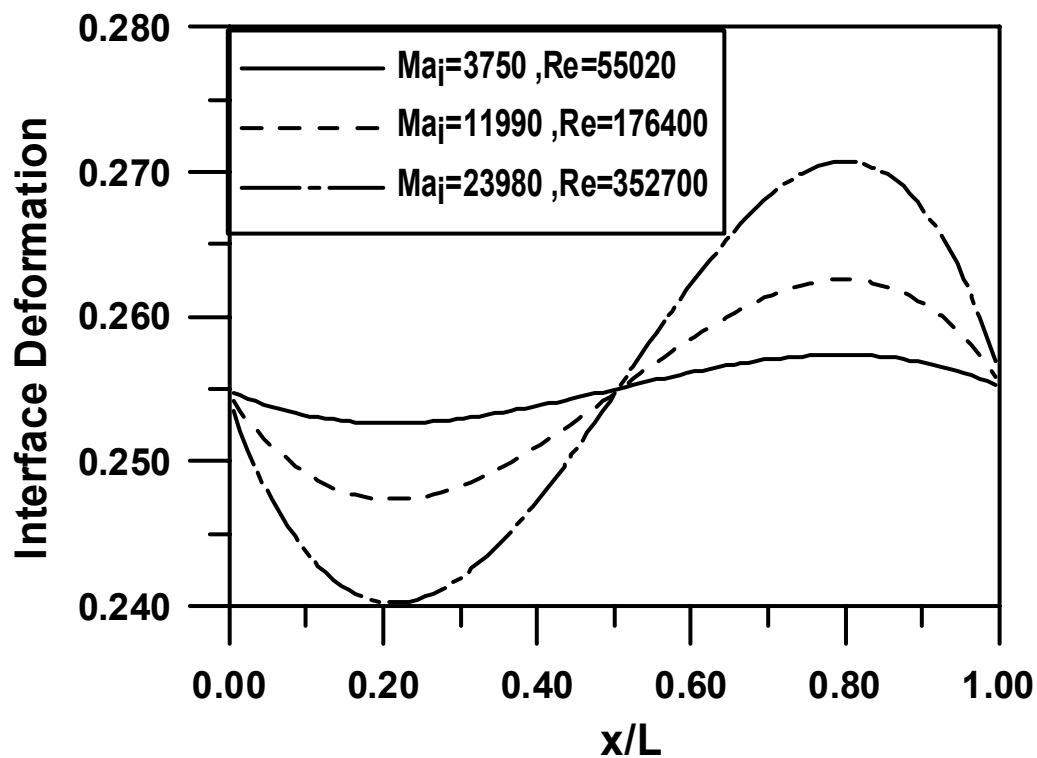


Fig.21. Interface deformation for different Ma_i at $A=L/H=2.0$.